ACADEMIC PRESS

Available online at www.sciencedirect.com

SCIENCE DIRECT®

DEVELOPMENTAL BIOLOGY

Developmental Biology 255 (2003) 206–215

www.elsevier.com/locate/ydbio

Sex-specific telomere redistribution and synapsis initiation in cattle oogenesis

Charlotte Pfeifer,[a] Harry Scherthan,[b] and Preben D. Thomsen[a,*]

[a] *Royal Veterinary and Agricultural University, Department of Anatomy and Physiology, Grønnegårdsvej 7, DK-1870 Frederiksberg C, Denmark*
[b] *MPI for Molecular Genetics, Ihnestrasse 73, D-14195 Berlin, Germany*

Received for publication 19 September 2002, revised 29 November 2002, accepted 2 December 2002

Abstract

The process of homolog pairing is well characterised in meiosis of male mammals, but much less information is available from female meiosis. We have therefore studied telomere dynamics by FISH and synapsis formation by immunostaining of synaptonemal complex proteins (SCP3, SCP1) on ovarian sections from 15 bovine fetuses, which covered the entire female prophase I. Telomeres displayed a dispersed intranuclear distribution in oogonia and relocated to the nuclear periphery during the preleptotene stage. Tight telomere clustering (bouquet formation) coincided with synapsis initiation at the leptotene/zygotene transition. Clustering of telomeres persisted during zygotene and even into the pachytene stage in a subset of nuclei, while it was absent in diplotene/dictyotene stage nuclei. Thus, the bouquet stage in the bovine female lasts significantly longer than in the male. Further, we observed that synapsis in the female initiated both terminally and interstitially in earliest zygotene stage oocytes, which contrasts with the predominantly terminal synapsis initiation in early zygotene spermatocytes of the bovine male. Altogether, our data disclose a sex-specific difference in telomere dynamics and synapsis initiation patterns in male and female bovine germ cells that may be related to the sex-specific differences in recombination rates observed in this and other mammalian species.

Keywords: Bovine; Oogenesis; Meiosis; Synapsis; Telomere; Sex-specific differences

Introduction

Homologous chromosomes (homologs) pair and recombine during the extended prophase of the first meiotic division. Pairing of homologs is associated with an intranuclear redistribution of chromosomes and the formation of the synaptonemal complex (SC), a proteinaceous structure that connects homologs along their lengths during the pachytene stage of meiotic prophase (Heyting, 1996; von Wettstein et al., 1984; Walker and Hawley, 2000). Recombination takes place within the context of the SC and, after dissolution of the SC during diplotene stage, homologs remain linked by chiasmata (for review see Jones, 1987; Roeder, 1997; Zickler and Kleckner, 1999). Although this general pattern of meiosis is shared between males and females, some sex-specific differences have been observed in mammals. At the global level, the total length of the SC is about twice the length in human oocytes compared to in spermatocytes (Bojko, 1983; Wallace and Hultén, 1985) and the overall recombination rates are about two times larger in females than in males in humans and mice (Broman et al., 1998; Roderick et al., 1996). This together with their own data on covariation of SC length and meiotic exchange rates led Lynn et al. (2002) to suggest that SC length reflects genetic map distance in mammals. The global sex-specific differences are also accompanied by differences in recombination rates between chromosomes and between chromosome regions. The terminal chromosome region is for example generally showing an increased recombination rate in males compared to females—a difference that seems to be reflected on the physical level by a corresponding difference in the frequency of chiasmata (Lawrie et al., 1995; Yu et al., 2001).

* Corresponding author. Fax: +45-35-28-25-47.
E-mail address: pdt@kvl.dk (P.D. Thomsen).

0012-1606/03/$ – see front matter © 2003 Elsevier Science (USA). All rights reserved.
doi:10.1016/S0012-1606(02)00093-3

Table 1
Occurrence of prophase stages as identified by immunostaining of SC proteins and telomere FISH

CRL (cm)	Age (d.p.c.)	Early Preleptotene	Late Preleptotene	Leptotene	Leptotene bouquet	Zygotene bouquet	Zygotene	Pachytene	Diplotene/ Dictyotene
6.0	60	−	−	−	−	−	−	−	−
9.4	70	+	−	−	−	−	−	−	−
9.6	70	−	−	−	−	−	−	−	−
13.5	80	+	+	+	−	+	+	+	−
14.5	85	+	+	+	−	+	+	+	−
16.0	90	+	+	+	+	+	−	+	−
16.5	90	+	+	+	+	+	+	+	−
17.0	90	+	+	+	−	+	+	+	+
19.0	95	−	−	+	+	−	+	+	−
20.0	95	−	+	+	+	+	+	+	−
22.5	105	+	+	+	+	+	+	+	+
35.0	140	−	−	+	+	+	+	+	+
40.0	150	+	+	+	+	+	+	+	+
46.0	160	−	−	−	−	−	−	−	+
51.0	165	+	+	+	−	+	+	+	+

Note. Age of fetuses are given in days after conception (d.p.c.) as estimated from fetal crown rump length (CRL; based on Rüsse and Sinowatz, 1991). The ages are assigned to 5-day intervals because of the variability of fetal sizes at a given d.p.c.

Given the sex-specific differences, it is unfortunate that the three-dimensional chromosome dynamics during first meiotic prophase has mainly been analysed using spermatocytes (Pfeifer et al., 2001; Rasmussen and Holm, 1978; Scherthan et al., 1996, 1998) and that most data on female prophase I have been obtained on squashed or microspread oocytes (e.g., human: Barlow and Hultén, 1998a; Speed, 1982, 1985; Wallace and Hultén, 1985; cattle: Koykul and Basrur, 1994; Koykul et al., 1997) where spatial information is lost. The three-dimensional reorganisation during onset of female prophase I has only been described in two ultrastructural studies using serial sectioning of few human oocytes (Bojko, 1983, 1985). Although the sample size is small, these studies indicated that the sex-specific differences of recombination rates may be reflected at the cytological level, because interstitial sites of synapsis initiation, which are expected to correlate with initiation of recombination (see Zickler and Kleckner, 1999), were observed only in human oocytes and not spermatocytes I (Bojko, 1983; Rasmussen and Holm, 1978).

We here report on the sequence of three-dimensional telomere redistribution and SC formation during first meiotic prophase in the bovine female as compared to that of bovine males.

Materials and methods

Bovine fetuses as well as 5 × 5 × 5 mm samples from adult bovine testes were collected approximately 20 min after slaughter at a local abattoir. Crown rump length (CRL) of each fetus was measured and the age of the fetus was estimated according to Rüsse and Sinowatz (1991) and the sex was diagnosed from the genitals. For each female fetus, ovaries were rapidly resected and one ovary was fixed for 4 h in 4% formaldehyde/PBS, while the contralateral ovary was snap frozen in isopentane, precooled in liquid N_2, and stored in liquid N_2 until use. Samples of testes of adult bulls were processed similarly.

Formaldehyde-fixed tissues were embedded in paraffin and 5 μm sections were mounted on silane-coated slides (Knittel Gläser, Germany) that were stored at 40°C over-

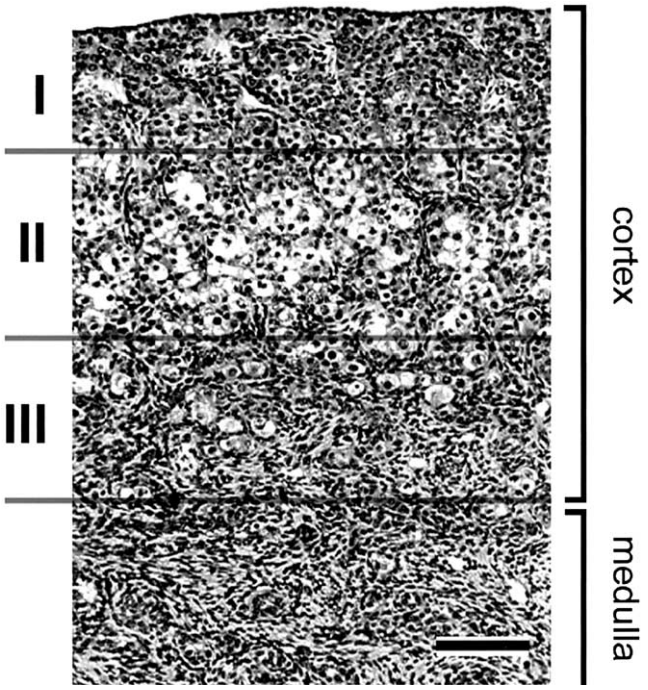

Fig. 1. Spatial organisation of germ cells in ovary of fetus at 95 dpc. The cortex is divided into three parts containing oogonia (I), germ cell clusters with oocytes in meiotic prophase (II), and diplotene/dictyotene stage oocytes in primordial follicles (III). HE staining of representative area beneath the germinal epithelium, bar, 100 μm.

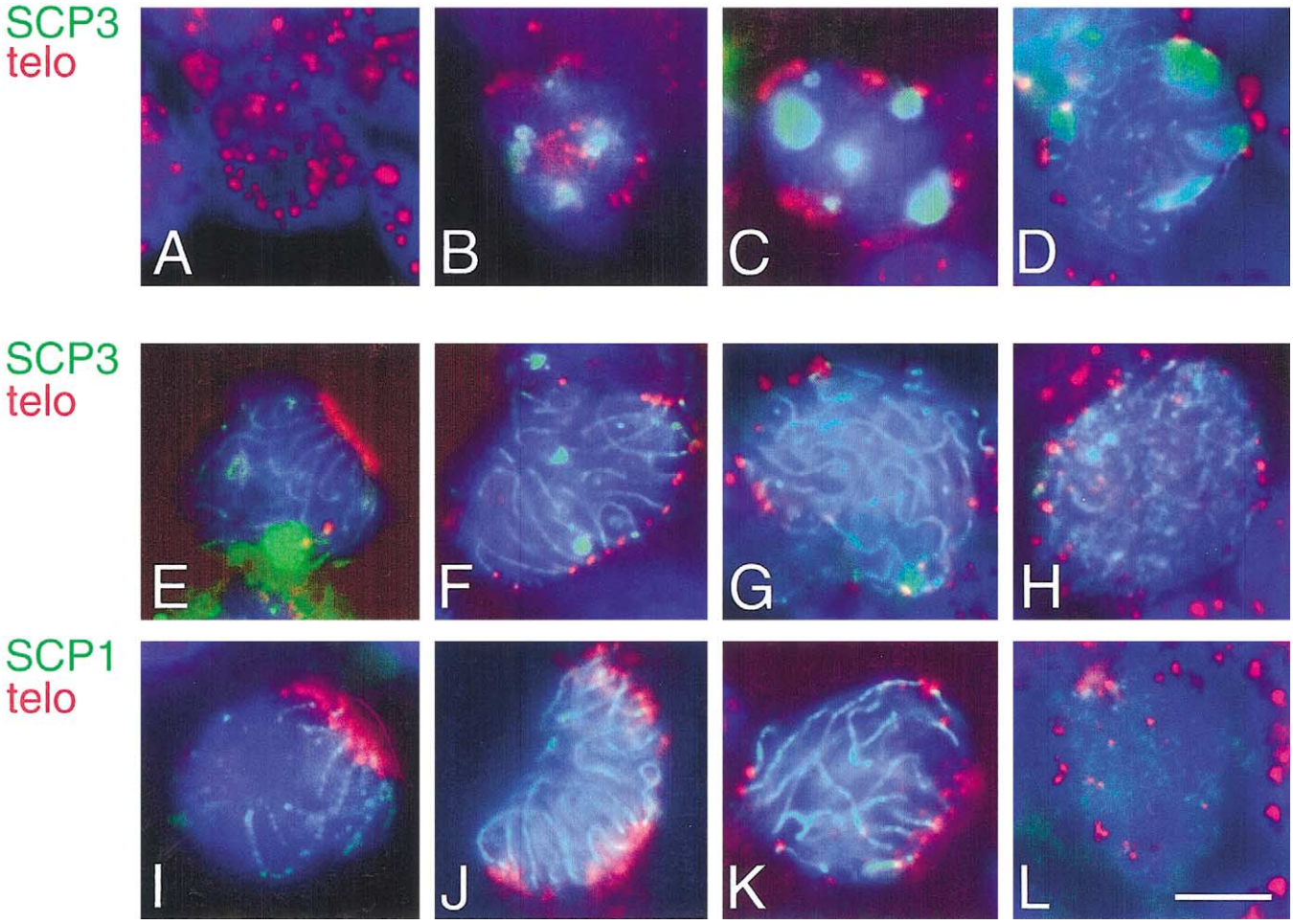

Fig. 2. Telomere distribution and assembly of axial elements and transverse filaments as revealed by telomere FISH and immunostaining of either SCP3 or SCP1 in cryosections of fetal bovine ovaries. (A–H) Nuclei of bovine oogonia and oocytes, focal planes at the nuclear equator. Telomeres (red), axial element protein SCP3 (green), DAPI (blue). Conventional fluorescence microscopy. (A) Nucleus of oogonium with perinuclear chromatin distribution and dispersed telomere signals. (B) Nucleus of early preleptotene stage oocyte with SCP3 foci and internal as well as peripheral telomeres. (C) Late preleptotene stage nucleus with several SCP3 foci and peripheral telomeres. (D) Leptotene stage oocyte with several SCP3 foci and elongate axial elements extending from the peripheral telomeres. (E) Leptotene/zygotene stage nucleus with tightly clustered telomeres at the nuclear periphery (bouquet), axial elements loop from the bouquet basis into the nuclear interior. One large aggregate is present. (F) Zygotene stage with partial telomere clustering at one side of the nucleus. Small aggregations of SCP3 are present. (G) Pachytene stage nucleus with peripheral telomeres and axial elements traversing the nucleus. SCP3 aggregates are absent. (H) Nucleus of early diplotene/dictyotene stage oocyte in primordial follicle (follicle cells outside frame). The axial elements are fragmented and telomeres are scattered throughout the nucleus. (I–L) Nuclei of bovine oocytes, focal planes at the nuclear equator. Telomeres (red), transverse filament protein SCP1 (green), DAPI (blue). (I) Early zygotene stage nucleus with telomere clustering (bouquet). Short peripheral and long interstitial stretches of SCP1–6 labelled SCs extend into the nucleus. (J) Crescent-shaped nucleus of zygotene/pachytene stage oocyte. Telomeres are partially clustered at one side of the nucleus and SCs are looping from the peripheral telomeres into the nucleus. (K) Pachytene stage nucleus with dispersed peripheral telomeres and SCs traversing the nuclear lumen. (L) Late diplotene/dictyotene stage oocyte in primordial follicle (follicle cells outside frame). Diffuse distribution of SCP1 protein and dispersed telomeres. Conventional fluorescence microscopy, bar, 5 μm.

night to foster firm adherence of tissue to the glass. Sections were stained with haematoxylin-eosin (HE) or by standard Feulgen procedure.

SC staining by SCP1 (Meuwissen et al., 1992) and SCP3 (Lammers et al. 1994) immunofluorescence was done as described previously (Pfeifer et al., 2001). The 12 μm frozen tissue sections were mounted on silane-coated glass slides and fixed in 4% formaldehyde/PBS. Sections not immediately used for immunostaining were stored in 80% glycerol/20% PBS at 4°C until further use. Combinatory SC IF and telomere FISH with a directly labelled $CCCATT_3$ PNA probe (DAKO) was done as described elsewhere (Pfeifer et al., 2001).

Apoptotic germ cells were identified by terminal deoxynucleotidyl transferase-mediated dUTP-digoxigenin nick end-labelling (TUNEL) method combined with immunostaining of SC proteins. Cryosections on silane-coated slides were permeabilised in 0.5% Triton/PBS for 90 min at RT, incubated with TdT buffer containing 100 U/ml TdT enzyme (Roche Biochem, Germany), 10 mM d(A,G,C)TP,

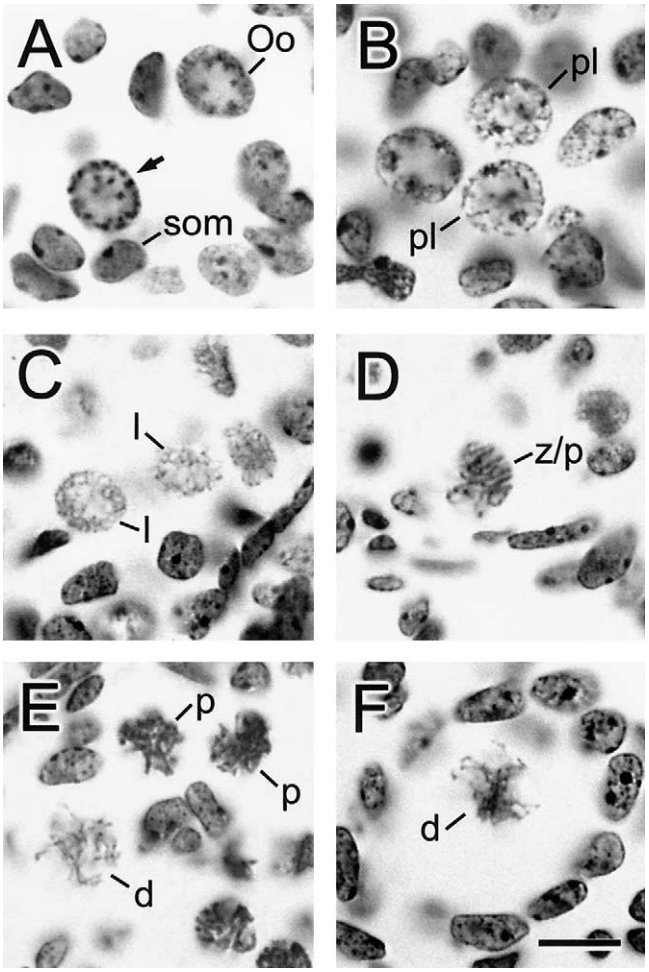

Fig. 3. Meiotic prophase stages in fetal bovine ovaries as revealed by Feulgen stain. (A) Oogonium (Oo) with perinuclear chromatin distribution, mitotic oogonium (arrow) with condensed chromosomes, and nuclei of somatic cells (som) with heterochromatin foci; fetus 60 dpc. (B) Preleptotene stage oocytes (p1), nuclei with chromocenters, and fine chromatin threads; fetus 70 dpc. (C) Leptotene stage oocytes (1), nuclei with fine chromosome threads; fetus 80 dpc. (D) Zygotene or early pachytene stage oocyte (z/p) with chromosomal bouquet; fetus 80 dpc. (E) Pachytene stage oocytes (p), nuclei with thick chromosome threads, diplotene/dictyotene stage oocyte (d) with faintly stained chromatin threads; fetus 80 dpc. (F) Diplotene/dictyotene stage oocyte (d) in primordial follicle; fetus 90 dpc. Bar, 10 μm.

and 10 mM digoxigenin-dUTP (Roche Biochem) for 2 h at 37°C followed by termination of the reaction by several washes in 2× SSC and PBS. Digoxigenin was detected using anti-DIG-Rhodamine (1:500; Roche Biochem), while immunostaining of SCP3 was performed as described above. Omission of either TdT or digoxigenin-dUTP from the TUNEL reaction produced no staining. The morphology of TUNEL-positive cells was examined by DAPI staining.

Preparations were evaluated using a Leica fluorescence microscope with separate band pass excitation filters for DAPI, FITC, and Cy3 and recorded using a Quantix CCD camera (Photometrix, Tucson AZ).

Results

We investigated meiotic chromosome behavior in female bovine fetuses of day 60 to day 165 postconception (pc) (Table 1). Since female meiosis begins at day 82 pc, in bovine fetuses and last divisions of oogonia take place around day 160 pc (Erickson, 1966; Rüsse, 1983), the material used spans the developmental window of the entire female prophase I. Accordingly, we observed that a distinct division of the ovarian cortex into an outer, a middle, and an inner region became evident from 80 to 95 days pc in HE-stained sections (Fig. 1). These regions were retained in all the following developmental stages, although their relative size changed. The proportion of the inner cortical region increased in the older age groups (105–165 dpc), while the proportion of the outer cortical region was reduced. We further observed a morphology of Feulgen-stained germ cell nuclei in fetal stages that corresponded well with previous descriptions of the normal germ cell development in fetal bovine ovaries (description included below).

Sections of the cryopreserved ovary were used for staging by FISH and immunostaining with SCP1 and SCP3. The section thickness of 12 μm represents a compromise between the aim to obtain nuclei that are largely intact (nuclei diameter ranged from 8 to 16 μm) and the requirement of efficient penetration of antibodies and probes. The description below is based on the analysis of 5–10 immunostained

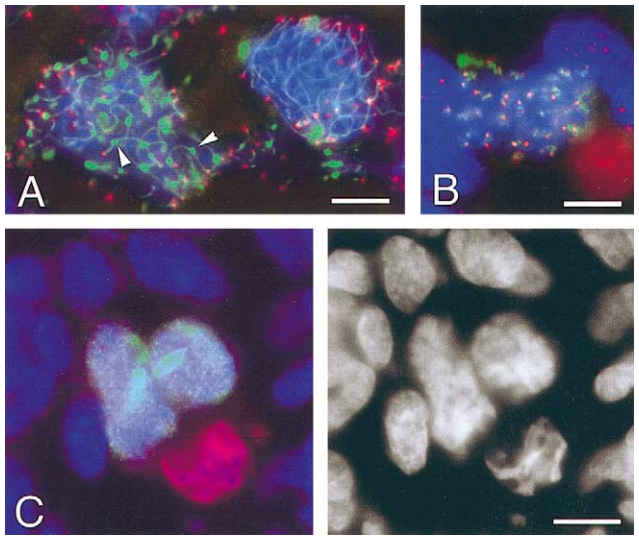

Fig. 4. Variant staining patterns in bovine oocytes. (A and B) Telomere FISH (red) and SCP3 immunostaining (green), DAPI (blue). C Combined immunostaining of SCP3 (green) and TUNEL (red). Nuclei (DNA) were counterstained with DAPI (blue). (A) Oocyte nucleus (left) with dot-like thickenings on SCP3-stained SCs (green, arrowheads) and leptotene stage nucleus (right) with peripheral telomeres (red), elongate axial elements and small SCP3 focus, fetus 105 dpc. (B) Oocyte nucleus (Z cell) with numerous dots/speckles of SCP3 (green) near and at the dispersed telomeres (red), fetus 165 dpc. (C) Germ cell cluster with three leptotene stage nuclei containing foci and stretches of SCP3 (green), and TUNEL-positive nucleus (red) with chromatin condensation, DAPI image of same area (right), fetus 165 dpc. Conventional fluorescence microscopy, bar, 5 μm.

ovarian sections for each fetus and of several focal planes of 10–50 representative nuclei of each substage and specimen.

Oogonia displayed an ellipsoid to round nucleus of 10-14μm diameter and perinuclear chromatin condensation in an otherwise weakly staining nucleus (Figs. 2A and 3A). They were found in the outer region of the ovarian cortex in all fetal stages studied. Telomeres were dispersed throughout the nuclear lumen and immunostaining for SC proteins was negative. Oogonia were easily distinguished from the surrounding somatic cells that were characterised by smaller ellipsoid nuclei (diameter 8–10 μm), a more diffuse chromatin distribution and one or more nucleoli (Fig. 3A) that presented themselves as characteristic dark areas in DAPI-stained sections (not shown).

A distinct cell type found in all Feulgen-stained fetal ovaries displayed a large, round nucleus with dense clusters of chromatin located predominantly at the nuclear periphery (Fig. 3A). We address this cell type as mitotic oogonia, because of their large size, peripheral chromatin distribution, and their presence in ovaries at 60 dpc—i.e., before the onset of meiosis. Furthermore, they are similar to the cells described as oocytes in premeiotic interphase in fetal bovine ovaries between 90 and 240 dpc (Henricson and Rajakoski, 1959), and as oogonia in mitotic prophase in the rat (Beaumont and Mandl, 1962). This interpretation is supported by the fact that they were generally TUNEL-negative, indicating that they were not degenerating oogonia, and the fact that SCP3 protein aggregates were absent. It is notable, however, that this variant morphology of mitotic oogonia seems to be specific for the female, because we did not observe similar features in bovine spermatogonia where mitotic figures displayed a central distribution of chromosomes.

Preleptotene stage nuclei were identified by the presence of one or more intranuclear SCP3 aggregates (Figs. 2B and C), which have been shown to mark the onset of prophase I in male cattle and mouse (Pfeifer et al., 2001; Scherthan et al., 1996). Early preleptotene stage oocytes were first observed in the ovary of fetuses at 70 dpc and late preleptotene stage oocytes at 80 dpc. Oocytes in preleptonema were present in fetuses at all following stages including 165 dpc. They were generally located in the outer region of the ovarian cortex. Nuclei were 12–13 μm and ellipsoid-round and contained fine chromatin threads and chromocenters in the Feulgen-stained sections (Fig. 3B). They stained evenly with DAPI but contained DAPI-negative areas, which colocalised with SCP3 aggregates. These areas correspond to nucleoli, since rDNA and SCP3 aggregates colocalise in mouse preleptotene spermatocytes (H. Scherthan and S. Weich, unpublished data). Nuclei with peripheral and internal telomeres (Fig. 2B) were interpreted as early preleptotene stage, whereas nuclei with telomeres exclusively dispersed over the nuclear periphery (Fig. 2C) were categorised as late preleptotene stage. This indicates a relocation of telomeres to the nuclear envelope during preleptotene stage, which mirrors the situation in the bovine male (Pfeifer et al., 2001) and the mouse (Scherthan et al., 1996) and even maize (Bass et al., 2000).

Leptotene oocytes were identified by the appearance of threads of SCP3-positive axial elements and SCP3 aggregates (Figs. 2D and E). Oocytes in leptonema were first observed in fetuses at 80 dpc and were present in fetuses at all following stages. They were mostly located in the germ cell clusters of the outer and middle cortical regions. Nuclei of leptone oocytes were round and larger (13–16 μm) than nuclei of preleptotene oocytes and the Feulgen-stained nuclei contained fine chromatin threads (Fig. 3C). As for preleptotene nuclei, they stained evenly with DAPI, with DAPI-dark areas at the regions of SCP3 aggregates (nucleoli). Telomeres were located exclusively at the nuclear periphery and were associated with short-to-long threads of SCP3-positive axial elements that extended from the peripheral telomeres to the nuclear interior. Leptotene nuclei with telomeres dispersed over the nuclear periphery (Fig. 2D) were interpreted as early leptotene, while leptotene nuclei with tightly clustered telomeres (bouquet arrangement) and more advanced axial element formation were categorised as late leptotene/earliest zygotene (Fig. 2E). Although leptotene stage oocytes generally failed to show SCP1 staining, there were a few nuclei with dispersed telomeres and one nucleus with clustered telomeres where a speckled SCP1 staining indicated synapsis initiation. These observations suggest that tight telomere clustering in the female commences at earliest zygotene.

Zygotene stage oocytes were identified by the appearance of intranuclear threads of SCP1 signals (Fig. 2I, F, and J). Both early and late zygotene stage oocytes were generally found in the germ cell clusters of the middle cortical region at 80 dpc and at all later stages. SCP1 aggregates were not observed prior to assembly into the SC. Generally, zygotene stage nuclei were crescent-shaped and smaller (9–12 μm) than those of leptotene stage oocytes. Nuclei at this stage further displayed SCP3 foci and elongated axial elements as well as peripherally located telomere signals. In early zygotene nuclei with short SCP1-positive threads, the telomere signals were tightly clustered at a small sector of the nuclear periphery (Fig. 2I). This bouquet topology was also observed in several Feulgen-stained nuclei (Fig. 3D). Synapsed regions appeared in the vicinity of the telomeres as well as interstitially (see below, Fig. 5). Later, zygotene nuclei with extended SC formation showed different degrees of telomere dispersion over the nuclear periphery (Fig. 2F and J). In the male, however, only one late zygotene nucleus of several hundred spermatocytes studied displayed telomere polarisation. Thus, the general pattern emerging from this and our previous study (Pfeifer et al., 2001) is that male zygotene nuclei show a shorter duration of the bouquet stage with less tight telomere clustering than females.

Pachytene stage oocytes displayed SCP3- and SCP1-positive SCs connected to the nuclear periphery by their telomeres and traversing the nucleus (Fig. 2G and K). Intranuclear SCP3 aggregates were no longer apparent. Oo-

cytes in pachynema were first observed in fetuses at 80 dpc and in all older fetuses. They were mostly located in germ cell clusters in the middle-to-inner regions of the ovarian cortex and their nuclei were displayed thick chromosome threads at Feulgen staining (Fig. 3E). The nuclei were crescent shaped to round, 12–15 μm in diameter, and evenly DAPI-stained. Telomere signals were located either clustered at one side of the nucleus (pachytene bouquet) or dispersed over the nuclear periphery, indicating a persistence of chromosome polarisation up to pachytene stage, which contrasts remarkably with the absence of telomere clustering in pachytene nuclei of the bovine male (Pfeifer et al., 2001).

Diplotene/dictyotene stage oocytes displaying a diffuse nuclear distribution of SCP3 and SCP1 (Fig. 2H and L) first appeared in fetuses at 90 dpc, became abundant at 105 dpc, and occurred at all later stages. Their nuclei were generally located in the inner region of the ovarian cortex and showed thin fuzzy chromatin threads upon Feulgen-staining (Fig. 3E and F). Generally, diplotene and (later) dictyotene oocytes located isolated in the centre of primordial follicles (Fig. 3F), although a few still occurred in germ cell clusters (Fig. 3E). The large (13–15 μm) and round nuclei showed weak DAPI-staining, and telomere signals were scattered throughout the nucleus. These nuclei were TUNEL-negative and we therefore address this staining pattern as a progressed dissolution of the SC and a low degree of chromatin packaging, possibly resulting from a high transcriptional activity during diplotene and dictyotene. Diplotene stage nuclei with separated SCP3-positive lateral axial elements, as present in the bovine male (Pfeifer et al., 2001), were not observed. The possibility that the fragile axial cores of the dismantling SC could have been disrupted by the IF+FISH technique cannot be neglected, since diplotene cores are known from spread rat oocytes (Dietrich et al., 1992). However, there remains the possibility that diplotene is a short transitory stage with rapid dissolution of SCs and SCP3 cores, which, by immunocytology, can hardly be discriminated from dictyotene. Therefore, we refer to nuclei with fragmenting SCs (Fig. 2H) as early and with a more diffuse distribution of SCP3 (Fig. 2L) as late and have included them in a combined diplotene/dictyotene category (Table 1).

Aberrant patterns, i.e., oocyte nuclei with staining patterns deviating from those described above, were a frequent finding. A variant SCP3 staining pattern was observed in two of the fetuses (105 and 150 dpc), where several nuclei showed SCP3-positive, dot-like thickenings distributed along the entire length of axial elements and/or SCs (Fig. 4A). Larger SCP3 foci not connected to axial/lateral elements were present in some nuclei and absent in others, while telomeres were consistently dispersed at the nuclear periphery. The SCP3-positive thickenings were distributed along the entire length of the axial/lateral elements with a difference in morphology than the SCP1-positive SC stretches in zygotene stage nuclei (see below). Thus, the SCP3 threads in these nuclei are unlikely to represent SC regions but they may rather be analogous to a type of leptotene stage human oocyte with nodular appearance of the thickened axial elements as described by Barlow and Hultén (1998a).

Nuclei containing fragmentary stretches of SCP3- or SCP1-positive threads were observed in ovaries from day 80 to 165 pc (Fig. 4B). The DAPI-stained morphology of these nuclei resembled leptotene or zygotene stage. A few nuclei furthermore displayed condensed chromatin divided into separate domains, which were labelled by SCP3 antibody in a speckled pattern. The fragmentary SC labelling patterns of these nuclei correspond well to the degenerative Z cells that have been observed in rat and human ovaries (Barlow and Hultén, 1998a; Beaumont and Mandl, 1962). However, none of the SCP3-positive cells showed a TUNEL-positive reaction and it remains to be determined whether they represent specific meiotic substages, such as early dictyate arrest, or whether they are early degenerative oocytes not yet showing a positive TUNEL-reaction.

In this context it is relevant to note that some of the cells in the germ cell clusters did show a positive TUNEL reaction (Fig. 4C). These nuclei, referred to as pycnotic by Ohno and Smith (1964), showed varying degrees of condensation and we therefore consider them degenerating (athretic) oocytes. This is an expected finding, since germ cell reduction in ovaries generally occurs by apoptosis among mitotic and meiotic populations (reviewed by Morita and Tilly, 1999).

Sex differences of synapsis initiation

The studies of SC formation in bovine fetal ovaries described above reveal differences in the pattern of synapsis initiation between bovine spermatocytes and oocytes (Pfeifer et al., 2001). To obtain a direct comparison of the pattern of synapsis initiation between three-dimensionally preserved bovine oocytes and spermatocytes I, cryosections of ovarian and testicular tissue were costained for SCP1 and telomeres. Early-to-mid zygonema was identified by stretches of SCP1-positive SC and clustered perinuclear telomeres. A total of 11 male and 20 female zygotene stage germ cells was analysed by recording two to five consecutive optical sections of each nucleus using conventional fluorescent microscopy.

In early zygotene spermatocytes I, numerous, and generally short, stretches of SCP1-positive SCs were located close to telomeres at the cluster site (Fig. 5A–C). Oocyte nuclei at this early stage of synapsis, in contrast, displayed only a few relatively long synapsed regions. The synapsed segments were detected near the peripheral telomeres as well as in the nuclear interior (Fig. 5D–F). The different intranuclear distribution between early zygotene oocytes and spermatocytes I shows that synapsis initiates predominantly near the peripheral telomeres at the nuclear envelope of spermatocytes, while synapsis commences at both terminally and interstitial regions in oocytes.

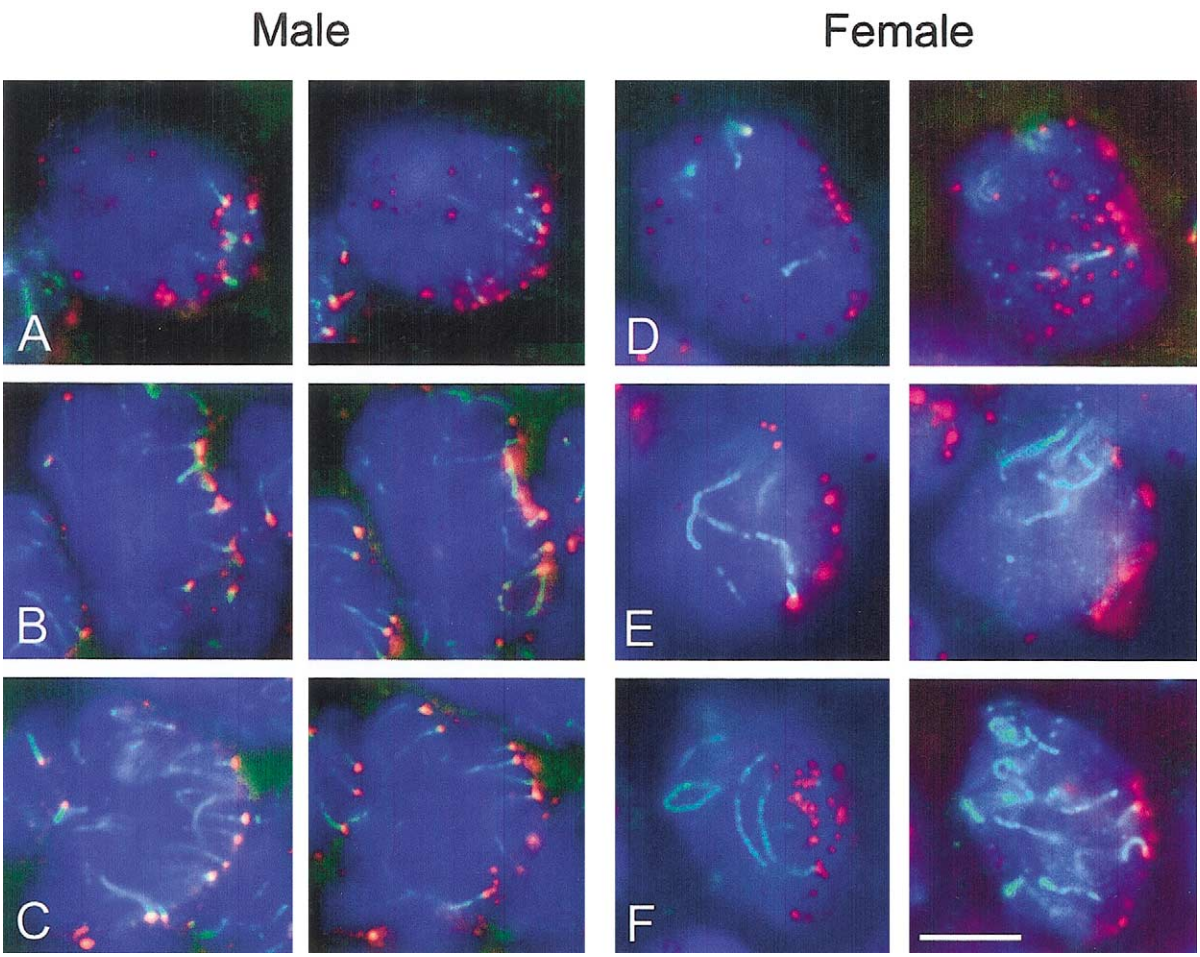

Fig. 5. Synapsis initiation as shown by immunostaining of transverse filament protein SCP1 (green) and telomere FISH (red) in cryosections of adult bovine testes and fetal bovine ovaries. Nuclei (DNA) were counterstained with DAPI (blue). (A–C) Nuclei of four selected zygotene stage spermatocytes, two focal planes shown for each nucleus. Telomeres are clustered at one side of the nucleus (bouquet). (A) Early zygotene stage nucleus with tight telomere clustering and short stretches of synapsed SC extending from the cluster site. (B), (C) Mid-zygotene stage nuclei with telomere clustering and elongate SCs stretches extending from most of the telomeres into the nuclear interior. (D–F) Nuclei of four selected zygotene stage oocytes, two focal planes shown for each nucleus. Telomeres are clustered at one side of the nucleus (bouquet). (D) Early zygotene stage nucleus with tight telomere clustering (at the top of the nucleus) and short stretches of synapsed SC in the nuclear interior as well as extending from the telomeres. (E), (F) Mid-zygotene nuclei with clustered telomeres and elongated SCs extending from a subset of telomeres at the cluster site and traversing the nucleus. Conventional fluorescence microscopy. Bar, 5 μm.

Discussion

We have investigated the occurrence of prophase I stages in the ovary of bovine fetuses using immunostaing of SC proteins in conjunction with telomere staining by PNA FISH. In agreement with histological studies (Erickson, 1966; Henricson and Rajakoski, 1959; Koykul and Basrur, 1994; Ohno and Smith, 1964; Rüsse, 1983), we observed that the outer region at the germinative epithelium contains mostly oogonia and preleptotene stage oocytes, whereas the well-developed ovigerous cords of the middle region are formed by germ cell clusters with oocytes in all stages of meiotic prophase. The germ cells of the inner region close to the medulla are primarily diplo- or dictyotene stage oocytes isolated in primordial follicles.

A direct comparison (Fig. 6) of the timing of synapsis initiation in male (Pfeifer et al., 2001) and female bovine germ cells (this study) reveals that initiation in oocytes, as visualised by SCP1 staining, coincides with tight clustering of telomeres (bouquet formation)—a timing which mirrors that of bouquet formation in spermatocytes of cattle and other mammals (Belar, 1928; Bojko, 1983; Pfeifer et al., 2001; Rasmussen and Holm, 1978; Scherthan et al., 1996), as well as species of different kingdoms (see Bass et al., 2000; Scherthan, 2001; Zickler and Kleckner, 1998). In contrast to the male, however, the telomere clustering in the cattle female is established during leptotene and persists during zygotene and even into early pachytene stage. Thus, bouquet dissolution is more rapid in the bovine male and occurs only during zygotene (Pfeifer et al., 2001). The significantly longer duration of the bouquet stage in female germ cells, as compared to males, leads us to suggest that tighter telomere clustering and a prolonged bouquet stage

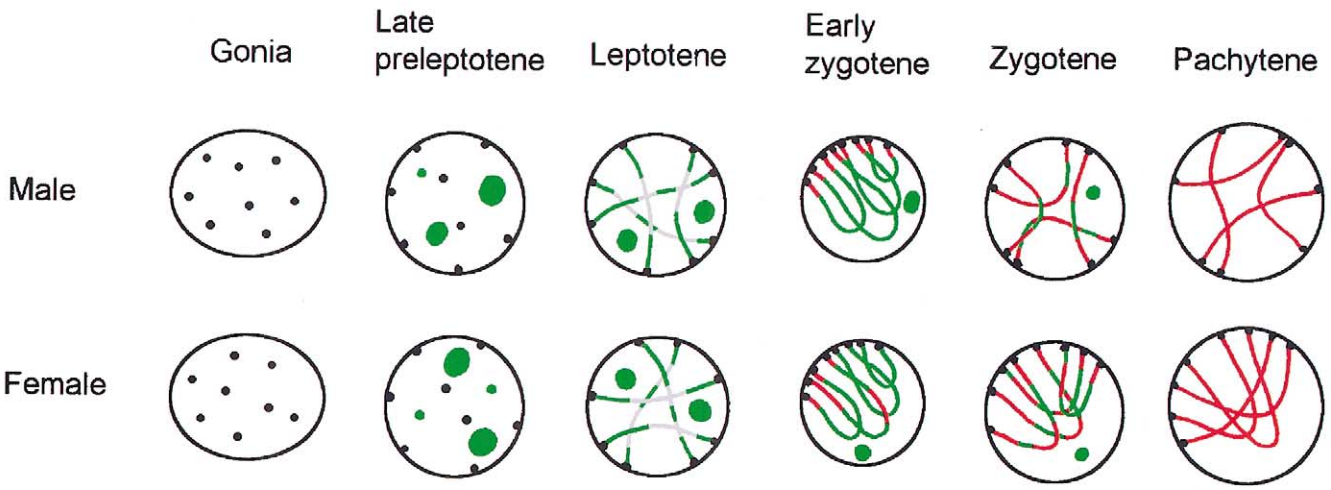

Fig. 6. Schematic representation of chromosome pairing and synapsis initiation in male and female bovine germ cells. In the male, chromosome polarisation is restricted to leptotene/zygotene and synapsis-initiation is terminal (Pfeifer et al., 2001), while in female cattle meiosis telomere clustering lasts into pachytene and synapsis initiates both terminally and interstitially. Telomeres are shown as black dots, SCP3 staining is illustrated in green and SCP1 staining is given in red.

during ovarian development contributes to prealignment and interstitial synapsis initiation in the female (see below).

In early preleptotene stage oocytes, intranuclear aggregates of SCP3 axial element protein appeared before the relocation of telomeres to the nuclear periphery, which mirrors the sequence in bovine spermatocytes (Pfeifer et al., 2001) but contrasts with findings in mouse spermatogenesis. In the latter, intranuclear SCP3 aggregates are first observed after telomeres have repositioned to the nuclear periphery (Scherthan et al., 1996). However, these variant observations in the two mammals may result from technical differences, because the mouse analysis was carried out on paraffin tissue sections (Scherthan et al., 1996) that may be less sensitive in the detection of smaller protein amounts than the cryosections used for the cattle analysis. Intranuclear SCP3 aggregates have also been observed in rat oogenesis (Dietrich et al., 1992) but their relation to telomere repositioning is currently not known.

In microspread human oocytes, immunostaining of SCP3 produces a distinctive labelling of axial cores and synapsed regions of the chromosomes, with weakly labelled unpaired axial elements and strongly labelled SCs (Barlow and Hultén, 1998a). This contrasts with the absence of such differences in tissue sections of bovine ovaries. Likewise, no difference has been described for intact nuclei of spermatocytes in cattle, mouse, and man (Pfeifer et al., 2001; Scherthan et al., 1996), which likely relates to a higher sensitivity of the spreading technique in fine-structure analysis of synapsis. Parallel IF analysis of male and female meiocytes revealed that, as judged by eye, the staining intensity of SCP3-positive axial elements in spermatocytes was always stronger than the intensity obtained in bovine oocytes. Similar sex differences have been observed in rat and have been suggested to reflect differences in the composition of the SC in relation to the greater complement length in oocytes versus spermatocytes (Dietrich et al., 1992). However, this seems unlikely the case in cattle, where the SCs are of approximately the same length in both sexes (Dollin et al., 1989; Koykul and Basrur, 1994).

We observed that synapsis predominantly initiates terminally in the male, whereas it initiates at both terminal and interstitial regions in the female. Similar differences in synapsis initiation in male and female meiocytes have been found in man: Three-dimensional reconstruction of serial sections from the electron microscope have shown that human spermatocytes display mainly telomeric synapsis initiation (Rasmussen and Holm, 1978), whereas both telomeric and interstitial synaptic pairing has been observed in human oocytes (Bojko, 1983). Studies by microspreading of human meiocytes have generally revealed synaptic pairing of homologs in terminal regions in both sexes (Barlow and Hultén, 1996, 1998a; Speed, 1988; Speed and Chandley, 1990; Wallace and Hultén, 1985), but a few interstitial initiation sites have been reported in oocytes (Barlow and Hultén, 1996; Wallace and Hultén, 1985).

It is conceivable that the sex differences in the chromosomal distribution of synapsis initiation may have functional consequences, since the number and distribution of MLH1 foci, a component of late recombination nodules that mark sites of crossing over (Baker et al., 1996), show a similar bias of distribution. In mouse and man, near-terminal MLH1 foci are more frequently observed in spermatocytes than in oocytes (Ashley and Plug, 1998; Barlow and Hultén, 1998b). This is in good agreement with the interstitial chiasmata distribution and general expansion of the genetic map in the interstitial chromosomal regions in females of human and mice (Hultén et al., 1995; Lawrie et al., 1995; Yu et al., 2001). The genetic maps from cattle have so far provided evidence for a sex difference of cattle chromosomes 1 and 21 (BTA1 and BTA21, respectively), which

both show an accumulation of recombination sites at telomeric regions in males (Barendse et al., 1993; Taylor et al., 1998). Other chromosomes such as BTA4, however, fail to display a sex difference in their genetic maps (Casas et al., 1999). This chromosomal variability should allow the testing of whether the sex differences of the genetic map are reflected in the chromosomal distribution of cytological markers of recombination.

Another consistent feature observed in early zygotene oocytes was the general presence of a few, relatively long synapsed segments, indicating advancement of synapsis between pairs of homologs before synapsis even starts in others. This distinctly asynchronous pattern was not observed in spermatocytes that generally displayed many short synapsed segments at early zygonema (Pfeifer et al., 2001). However, a more detailed analysis will be necessary to elucidate whether the asynchronous synapsis initiation and progression is a random process or whether it preferentially involves certain homolog pairs as has been observed in other species (see Scherthan and Schonborn, 2001 and references therein). Finally, it will be interesting to see whether the pronounced asynchrony in synapsis in females has any bearing on the incidence of synaptic errors, which seems to be tolerated in higher numbers in females as compared to males (Hunt and Hassold, 2002; Yuan et al., 2002; Koykul and Basrur, 1994; Dollin et al., 1989).

Acknowledgments

We thank Christa Heyting for the generous gift of antibodies, and Anne Friis Petersen and Gunnel Holden for competent technical assistance. C.P. was supported by a Ph.D. grant from the Royal Veterinary and Agricultural University. P.D.T. acknowledges support from the Danish Biotechnology Instrument Center and H.S. acknowledges support from the DFG (SCHE 350/8-3).

References

Ashley, T., Plug, A., 1998. Caught in the act: deducing meiotic function from protein immunolocalization. Curr. Top. Dev. Biol. 37, 201–239.

Baker, S.M., Plug, A.W., Prolla, T.A., Bronner, C.E., Harris, A.C., Yao, X., Christie, D.M., Monell, C., Arnheim, N., Bradley, A., Ashley, T., Liskay, R.M., 1996. Involvement of mouse Mlh1 in DNA mismatch repair and meiotic crossing over. Nat. Genet. 13, 336–342.

Barendse, W., Armitage, S.M., Kirkpatrick, B.W., Moore, S.S., Georges, M., Womack, J.E., Hetzel, J., 1993. A genetic map of index DNA loci on bovine chromosome 21. Genomics 18, 598–601.

Barlow, A.L., Hultén, M.A., 1996. Combined immunocytogenetic and molecular cytogenetic analysis of meiosis I human spermatocytes. Chromosome Res. 4, 562–573.

Barlow, A.L., Hultén, M.A., 1998a. Combined immunocytogenetic and molecular cytogenetic analysis of meiosis I oocytes from normal human females. Zygote 6, 27–38.

Barlow, A.L., Hultén, M.A., 1998b. Crossing over analysis at pachytene in man. Eur. J. Hum. Genet. 6, 350–358.

Bass, H.W., Riera-Lizarazu, O., Ananiev, E.V., Bordoli, S.J., Rines, H.W., Phillips, R.L., Sedat, J.W., Agard, D.A., Cande, W.Z., 2000. Evidence for the coincident initiation of homolog pairing and synapsis during the telomere-clustering (bouquet) stage of meiotic prophase. J. Cell Sci. 113, 1033–1042.

Beaumont, H.M., Mandl, A.M., 1962. A quantitative and cytological study of oogonia and oocytes in the foetal and neonatal rat. Proc. R. Soc. Lond. B Biol. Sci. 155, 557–579.

Belar, K., 1928. Chromosomenreduktion. Die cytologischen Grundlagen der Vererbung, in: Baur, E., Hartmann, M. (Eds.), Handbuch der Vererbungswissenschaft, Vol. 1, Geb. Borntraeger, Berlin, pp. 168–201.

Bojko, M., 1983. Human meiosis VIII. Chromosome pairing and formation of the Synaptonemal Complex in oocytes. Carlsberg Res. Commun. 48, 457–483.

Bojko, M., 1985. Human meiosis IX. Crossing over and chiasma formation in oocytes. Carlsberg Res. Commun. 50, 43–72.

Broman, K.W., Murray, J.C., Sheffield, V.C., White, R.L., Weber, J.L., 1998. Comprehensive human genetic maps: individual and sex-specific variation in recombination. Am. J. Hum. Genet. 63, 861–869.

Casas, E., Barendse, W., Beever, J.E., Burns, B.M., Davis, S.K., Erhardt, G., Forster, M., Gomez-Raya, L., Kalm, E., Kappes, S.M., Klungland, H., Lewin, H.A., Lien, S., Olsaker, I., Reinsch, N., Schwerin, M., Song, Y., Taylor, J.F., Thomsen, H., Våge, D.I., Wu, X., Xu, N., Yeh, C.C., 1999. Bovine chromosome 4 workshop: consensus and comprehensive linkage maps. Anim. Genet. 30, 375–377.

Dietrich, A.J.J., Kok, E., Offenberg, H.H., Heyting, C., de Boer, P., Vink, A.C.G., 1992. The sequential appearance of components of the synaptonemal complex during meiosis of the female rat. Genome 35, 492–497.

Dollin, A.E., Murray, J.D., Gillies, C.B., 1989. Synaptonemal complex analysis of hybrid cattle. I. Pachytene substaging and the normal full bloods. Genome 32, 856–864.

Erickson, B.H., 1966. Development and radioresponse of the prenatal bovine ovary. J. Reprod. Fertil. 11, 105.

Henricson, B., Rajakoski, E., 1959. Studies of oocytogenesis in cattle. Cornell Vet. 49, 494–503.

Heyting, C., 1996. Synaptonemal complex: structure and function. Curr. Op. Cell Biol. 8, 389–396.

Hultén, M.A., Tease, C., Lawrie, N.M., 1995. Chiasma-based genetic map of the mouse X chromosome. Chromosoma 104, 223–227.

Hunt, P.A., Hassold, T.J., 2002. Sex matters in meiosis. Science 296, 2181–2183.

Jones, G.H., 1987. Chiasmata, in: Moens, P.B. (Ed.), Meiosis, Academic Press, Orlando, pp. 213–244.

Koykul, W., Basrur, P.K., 1994. Synaptic anomalies in fetal bovine oocytes. Genome 37, 83–91.

Koykul, W., Switonski, M., Basrur, P.K., 1997. The X bivalent in fetal bovine oocytes. Hereditas 126, 59–65.

Lammers, J.H.M., Offenberg, H.H., van Aalderen, M., Vink, A.C.G., Dietrich, A.J.J., Heyting, C., 1994. The gene encoding a major component of the Lateral Elements of Synaptonemal Complexes of the rat is related to X-linked lymphocyte-regulated genes. Mol. Cell Biol. 14, 1137–1146.

Lawrie, N.M., Tease, C., Hultén, M.A., 1995. Chiasma frequency, distribution and interference maps of mouse autosomes. Chromosoma 140, 308–314.

Lynn, A., Koehler, K.E., Judies, L., Chan, E.R., Cherry, J.P., Schwartz, S., Seftel, A., Hunt, P.A., Hassold, T.J., 2002. Covariation of synaptonemal complex length and mammalian meiotic exchange rates. Science 296, 2222–2225.

Meuwissen, R.L., Offenberg, H.H., Dietrich, A.J., Riesewijk, A., van Iersel, M., Heyting, C., 1992. A coiled-coil related protein specific for synapsed regions of meiotic prophase chromosomes. EMBO J. 11, 5091–5100.

Morita, Y., Tilly, J.L., 1999. Oocyte apoptosis: like sand through an hourglass. Dev. Biol. 213, 1–17.

Ohno, S., Smith, J.B., 1964. Role of fetal follicular cells in meiosis of mammalian oöcytes. Cytogenetics 3, 324–333.

Pfeifer, C., Thomsen, P.D., Scherthan, H., 2001. Centromere and telomere redistribution precedes homologue pairing and terminal synapsis initiation during prophase I of cattle spermatogenesis. Cytogenet. Cell Genet. 93, 304–314.

Rasmussen, S.W., Holm, P.B., 1978. Human meiosis II. Chromosome pairing and recombination nodules in human spermatocytes. Carlsberg Res. Commun. 43, 275–327.

Roderick, T.H., Hillyard, A.L., Maltais, L.J., Blake, C.S., 1996. Recombination percentages and chromosomal assignments, in: Lyon, M.F., Rastan, S., Brown, S.D.M. (Eds.), Genetic Variants and Strains of the Laboratory Mouse, third ed., Oxford Univ. Press, Oxford, pp. 929–1255.

Roeder, G.S., 1997. Meiotic chromosomes: it takes two to tango. Genes Dev. 11, 2600–2621.

Rüsse, I., 1983. Oogenesis in cattle and sheep. Bibl. Anat. 24, 77–92.

Rüsse, I., Sinowatz, F., 1991. Lehrbuch der Embryologie der Haustiere. Verlag Paul Parey, Berlin.

Scherthan, H., 2001. A bouquet makes ends meet. Nat. Rev. Mol. Cell Biol. 2, 621–627.

Scherthan, H., Eils, R., Trelles-Sticken, E., Dietzel, S., Cremer, T., Walt, H., Jauch, A., 1998. Aspects of three-dimensional chromosome reorganization during the onset of human male meiotic prophase. J. Cell Sci. 111, 2337–2351.

Scherthan, H., Schönborn, I., 2001. Asynchroneous chromosome pairing in male meiosis of the rat (*Rattus norvegicus*). Chromosome Res. 9, 273–282.

Scherthan, H., Weich, S., Schwegler, H., Heyting, C., Härle, M., Cremer, T., 1996. Centromere and telomere movements during early meiotic prophase of mouse and man are associated with the onset of chromosome pairing. J. Cell Biol. 134, 1109–1125.

Speed, R.M., 1982. Meiosis in the foetal mouse ovary. Chromosoma 85, 427–437.

Speed, R.M., 1985. The prophase stages in human foetal oocytes studied by light and electron microscopy. Hum. Genet. 69, 69–75.

Speed, R.M., 1988. The possible role of meiotic pairing anomalies in the atresia of human fetal oocytes. Hum. Genet. 78, 260–266.

Speed, R.M., Chandley, A.C., 1990. Prophase of meiosis in human spermatocytes analysed by EM microspreading in infertile men and their controls and comparisons with human oocytes. Hum. Genet. 84, 547–554.

Taylor, J.F., Eggen, A., Aleyasin, A., Armitage, S.M., Barendse, W., Beever, J.E., Bishop, M.D., Brenneman, R.A., Burns, B.M., Davis, S.K., Elo, K., Harlizius, B., Kappes, S.M., Keele, J.W., Kemp, S.J., Kirkpatrick, B.W., Lewin, H.A., Ma, R.Z., McGraw, R.A., Pomp, D., Stone, R.T., Sugimoto, Y., Teale, A.J., Vaiman, D., Zanotti, M.C., 1998. Report of the first workshop on the genetic map of bovine chromosome 1. Anim. Genet. 29, 228–235.

von Wettstein, D., Rasmussen, S.W., Holm, P.B., 1984. The synaptonemal complex in genetic segregation. Ann. Rev. Genet. 18, 331–413.

Walker, M.Y., Hawley, R.S., 2000. Hanging on to your homolog: the roles of pairing, synapsis and recombination in the maintenance of homolog adhesion. Chromosoma 109, 3–9.

Wallace, B.M., Hultén, M.A., 1985. Meiotic chromosome pairing in the normal human female. Ann. Hum. Genet. 49 (Pt. 3), 215–226.

Yu, A., Zhao, C., Fan, Y., Jang, W., Mungall, A.J., Deloukas, P., Olsen, A., Doggett, N.A., Ghebranious, N., Broman, K.W., Weber, J.L., 2001. Comparison of human genetic and sequence-based physical maps. Nature 409, 951–953.

Yuan, L., Liu, J.G., Hoja, M.R., Wilbertz, J., Nordqvist, K., Hoog, C., 2002. Female germ cell aneuploidy and embryo death in mice lacking the meiosis-specific protein SCP3. Science 296, 1115–1118.

Zickler, D., Kleckner, N., 1999. Meiotic chromosomes: integrating structure and function. Annu. Rev. Genet. 33, 603–754.